RSC Sustainability

ROYAL SOCIETY OF CHEMISTRY

PAPER

View Article Online
View Journal

Cite this: DOI: 10.1039/d5su00465a

Sustainable valorization of mandarin peel waste into multifunctional cellulose/pectin/PVA films with superior mechanical and UV-blocking performance

Yongjun Cho, Sunoo Hwang, Pham Thanh Trung Ninh, Youngju Kim, Shinhyeong Choe and Jaewook Myung *

Biodegradable polymers offer a promising solution to global plastic pollution. However, commercial options such as poly(butylene adipate-*co*-terephthalate) (PBAT) and poly(lactic acid) (PLA) often rely on petroleum-based feedstocks or costly microbial production. Lignocellulosic biomass presents a sustainable alternative, yet a substantial amount is discarded, and its utilization remains limited. In this study, we present a more sustainable and cost-effective approach to fabricating biodegradable plastic films from mandarin (*Citrus reticulata* Blanco) peel waste. Using a simple, one-step process with aqueous sodium carbonate as a mild pretreatment reagent, we partially hydrolyze the mandarin peel structure while simultaneously blending it with poly(vinyl alcohol) (PVA). To further enhance functionality, additional post-treatments including ultrasonication and washing are employed. The optimized films demonstrate excellent tensile strength (~60 MPa), near-complete UV-blocking (~100%), and strong antioxidant activity (~54% radical scavenging). Furthermore, the films exhibit outstanding oxygen barrier properties and enhanced water vapor barrier properties. Finally, biodegradation under simulated river water and soil conditions, as well as soil ecotoxicity assessments, confirms the products' minimal environmental impact in various end-of-life scenarios. These findings highlight the potential of the developed material for packaging and agricultural mulch applications, addressing both plastic waste pollution and biomass valorization.

Received 23rd June 2025
Accepted 1st November 2025

DOI: 10.1039/d5su00465a

rsc.li/rscsus

Sustainability Spotlight

A sustainable transition to biodegradable plastics derived from low-value feedstocks is crucial to addressing the global plastic pollution crisis. Our work presents an efficient valorization strategy that upcycles mandarin peel waste into biodegradable and multifunctional bioplastics. Using a one-step Na_2CO_3-mediated mild base treatment, we simultaneously achieve partial hydrolysis of lignocellulose, PVA dissolution, and polymer blending. This method eliminates the need for toxic chemicals or energy-intensive procedures, adhering to multiple principles of green chemistry, including waste prevention, safer solvents, and energy efficiency. Our approach advances sustainable materials innovation while minimizing environmental burden, contributing to the UN Sustainable Development Goals (SDGs): SDG 12 (Responsible Consumption and Production), SDG 14 (Life Below Water), and SDG 15 (Life on Land).

Introduction

Plastic is cheap, durable, and easily processable, and therefore has been widely used in diverse fields such as packaging, construction, textiles, and agriculture. As a result, global plastic waste generation is projected to rise from 353 Mt in 2019 to 1014 Mt by 2060.[1] Despite the increasing effort on recycling,[2] most plastic waste is mismanaged through incineration, landfill, or dumping.[3] This situation is exacerbating environmental pollution by producing micro- and nanoplastics,[4] threatening multiple UN Sustainable Development Goals. Therefore, a shift towards biodegradable materials is essential for a sustainable society.[5] Although biodegradable polymers have been proposed as a solution, their widespread commercialization remains limited. Most bioplastics are either still expensive (produced from microbial synthesis, *e.g.*, PLA) or have a high carbon footprint due to fossil-based production (*e.g.*, PBAT).[6–9] In addition, many so-called biodegradable polymers do not fully biodegrade under all environmental conditions, often requiring elevated temperatures and humidity for complete breakdown.[10]

A waste valorization strategy offers an eco-friendly alternative to mitigating plastic pollution. Biomass waste is an abundant and cost-effective feedstock rich in valuable chemicals,[11,12] generated from various natural and human activities, including forestry, agriculture, and the food industry. Among these

Department of Civil and Environmental Engineering, KAIST, Daejeon 34141, Republic of Korea. E-mail: jjaimyung@kaist.ac.kr

applications, bioplastic is a high-value product that can be readily produced through straightforward valorization methods due to its high natural polymer content.[13] However, bioplastic preparation methods with insufficient pretreatment often result in poor mechanical strength,[14] while the direct use of biomass waste as a filler underutilizes its valorization potential. Therefore, effective and sustainable pretreatment methods—such as lignocellulose regeneration, selective extraction of polymers, or polymer blending—are essential for enhancing bioplastic performance.[15,16] Among these approaches, one popular approach is the extraction of nanocellulose sourced from cellulose-rich materials such as wood,[17] cotton,[18] sugarcane bagasse,[19] and agricultural residue.[20] While nanocellulose provides excellent mechanical strength, its production often requires multiple energy-demanding steps and/or the use of toxic solvents such as sulfuric acid. Moreover, when utilizing materials with low cellulose content, cellulose extraction can generate a considerable amount of waste.

To address these challenges, *in situ* fibrillation and regeneration of lignocellulose have recently gained attention. These approaches employ mild pretreatment reagents and fewer processing steps with lower energy consumption, while maintaining excellent mechanical properties.[21] In one example, citrus peel was valorized into bioplastic by a two-step delignification, glycerol addition, ultrasonication, and post-crosslinking with calcium chloride.[22] While this approach demonstrated robust pectocellulosic film products and emulsifiers derived from by-products, the overall procedure required multiple reaction and separation steps, and the tensile properties were assessed only after an additional hot-pressing process. Another study utilized spent coffee grounds to fabricate composite films by incorporating dissolving pulp with *N*-methylmorpholine-*N*-oxide as a solvent.[16] The resulting films exhibited good mechanical properties and UV-blocking ability; however, their tensile strength was decreased with increasing spent coffee ground content. More recent studies have utilized spinach stems, peanut shells, and grass biomass to produce bioplastics through a simple, zero-waste process using aqueous ammonium hydroxide at ambient temperatures (30–40 °C).[23,24] Although *in situ* cellulose micro- and nanofibrillation was proposed as a potential advantage, this method had several drawbacks, including a long reaction time (24 hours), the use of irritating ammonium hydroxide, and the need for an additional blending step with thermoplastic starch in the case of peanut shells. Therefore, a more energy-efficient and straightforward pretreatment method for producing high-quality bioplastics from agricultural waste remains a critical research goal.

In this study, mandarin (*Citrus reticulata* Blanco) peel waste was chosen as a model biomass due to its global annual production of approximately 31.6 million tons.[25] Citrus fruit peels are rich in pectin and essential oils (*e.g.*, polyphenols, carotenoids, and limonene) and contain relatively low amounts of lignin and cellulose, distinguishing them from common agricultural wastes.[26,27] These characteristics enable citrus peel powder to disperse easily in water while providing additional functionalities such as UV-blocking and antioxidant properties. Additionally, utilizing mandarin peel waste for bioplastics remains a relatively unexplored research area,[26] with only a few studies focusing on its blending with poly(vinyl alcohol) (PVA).[28,29] PVA is an excellent candidate for blending with natural polymers, as it enhances material applicability while retaining biodegradability.[30] Although derived from poly(vinyl acetate), a petroleum-based polymer, PVA is inexpensive and biodegradable in various natural environments, including aqueous environments, due to its high hydroxyl group content. Besides, the water-soluble nature of PVA improves its compatibility with natural polymers and facilitates processing *via* solvent casting, making it a versatile polymer for biodegradable plastic formulations.[31–35]

Herein, we propose a facile one-step mild base pretreatment, in which mandarin peel is treated with sodium carbonate (Na_2CO_3) solution while simultaneously blending with PVA. Although Na_2CO_3 has previously been employed to extract microcellulose from sugarcane bagasse,[19] this study is the first to explore its application in mandarin peel pretreatment and *in situ* conversion into biodegradable plastic. We postulated that (1) blending natural polymers with PVA could exhibit synergistic effects through intermolecular hydrogen bonding (Fig. S1); (2) the mandarin peel to PVA (M/P) ratio can be tailored for balancing waste valorization efficiency and product's properties. We first present the optimization strategies for fabricating mandarin peel/PVA blend films (M/P films), and then evaluate their functional properties, including mechanical strength, antioxidant activity, gas barrier properties, and biodegradability.

Experimental

Chemicals

Commercial mandarin peel powder, produced by simple drying and pulverization (Jangmung Food, Republic of Korea), was stored in a 50 °C oven to remove residual moisture and filtered with a 250 μm sieve before use. The following chemicals were obtained from Sigma-Aldrich (United States): PVA (product no. 341584, M_w = 89 000–98 000 g mol^{-1}, degree of hydrolysis: >99%), sodium carbonate (Na_2CO_3), sodium hydroxide (NaOH), glycerol, acetic acid, sodium chlorite, dimethyl sulfoxide-d_6 (DMSO-d_6), α-cellulose (product no. C8002), monopotassium phosphate (KH_2PO_4), ammonium hydroxide (NH_4Cl), magnesium sulfate ($MgSO_4$), sodium nitrate ($NaNO_3$), and urea ($CO(NH_2)_2$). Anhydrous calcium chloride and 1 M hydrochloric acid solution were acquired from Samchun Chemicals (Republic of Korea), and anhydrous ethanol was obtained from Duksan Pure Chemicals (Republic of Korea). Low-density polyethylene (LDPE) film (LB7500N, LG Chem, Republic of Korea) was kindly provided by Yonsei University and utilized as a negative control in the biodegradation test.

Fabrication of M/P films *via* different pretreatment methods

To examine the effect of different pretreatment methods, three production routes were employed while maintaining a 1 : 1 mass ratio of mandarin peel to PVA (Fig. S2). Glycerol (40 wt% of the starting materials) was added as a plasticizer, as its absence prevented successful film removal. The sample codes were designated by the pretreatment method and the mandarin peel/

Table 1 Summary of mandarin peel/PVA (M/P) film formulations[a]

	Concentration of components (g/100 mL solvent)				
Sample code	Mandarin peel	PVA	Glycerol	Pretreatment	Post-treatment
Na_2CO_3-1:1	5	5	4	Aqueous Na_2CO_3 hydrolysis	—
Na_2CO_3-1:2	3.33	6.67	4	Aqueous Na_2CO_3 hydrolysis	—
Na_2CO_3-1:4	2.5	7.5	4	Aqueous Na_2CO_3 hydrolysis	—
Delig-1:1	6.67	6.67	5.33	Two-step delignification	—
Water-1:1	5	5	4	Hot water dispersion	—
Na_2CO_3-1:1-U	5	5	0	Aqueous Na_2CO_3 hydrolysis	Ultrasonication
Na_2CO_3-1:1-W	5	5	0	Aqueous Na_2CO_3 hydrolysis	Ultrasonication, washing
Na_2CO_3-1:2-W	3.33	6.67	0	Aqueous Na_2CO_3 hydrolysis	Ultrasonication, washing
Na_2CO_3-1:4-W	2.5	7.5	0	Aqueous Na_2CO_3 hydrolysis	Ultrasonication, washing
PVA	0	10	0	Hot water dispersion	—

[a] —: Not performed.

PVA (M/P) blend ratio (Table 1). The final thickness of films was measured using a micrometer (Model no. 700-118-20, Mitutoyo, Japan), which was maintained at ~0.20 mm. In addition, pure PVA films were also produced by dissolving PVA powder in deionized water (10 w/v%), stirring at 90 °C for complete dissolution, and casting. Detailed procedures for sample characterization are provided in the SI.

Na_2CO_3-mediated hydrolysis. The following procedure was adapted from the literature,[23] with the replacement of the original solvent by aqueous Na_2CO_3. Predetermined amounts of mandarin peel and PVA powder were mixed into a 1 w/v% Na_2CO_3 solution. The solution was stirred at 90 °C for 3 hours to dissolve PVA and partially hydrolyze the lignocellulose structure, after which glycerol was added dropwise. The final solution was then filtered, cast onto a hydrophobic substrate (glass or stainless steel), and dried at room temperature for 2 days to obtain the Na_2CO_3-1:1 sample.

Delignification followed by PVA blending. Mandarin peel powder was initially delignified through a two-step process as reported elsewhere,[22] and PVA was subsequently blended (Fig. S3). Briefly, 10 g of mandarin peel was dispersed in 150 mL of 10 vol% ethanol solution at 90 °C for 2 hours, then centrifuged. While keeping the pectin-rich supernatant in a refrigerator, the filtered solid was treated with 150 mL of 1 M NaOH solution at 90 °C for 2 hours, and then filtered and washed to remove lignin. After that, the remaining cellulose-rich solid was mixed with the supernatant from the first step, followed by the addition of PVA (10 g) and glycerol, and mixed at 90 °C for 2 hours. Finally, the solution was cast and dried at room temperature for 2 days to produce the Delig-1:1 sample.

Hot water dispersion. For the control sample (Water-1:1), mandarin peel, PVA, and glycerol were added to deionized water and mixed at 90 °C for 2 hours, followed by casting.

Fabrication of M/P films with additional post-treatments

Additional treatments were introduced to improve the properties of the products. First, mandarin powder and PVA were subjected to the Na_2CO_3 pretreatment as described above, albeit without glycerol addition. After cooling to room temperature, ultrasonication was performed at 800 W for 10 minutes in pulse mode (5 seconds on, 1 second off) using an ice bath, stirred for an additional 20 minutes for degassing, and then finally cast. Thereafter, the dried film was washed several times with water until the washing liquid became clear, and dried again. The films with different M/P ratios were prepared *via* the same procedure. The 1 : 1 ratio-based film (Na_2CO_3-1:1-W) was further utilized for thermal analysis, as well as antioxidant and biodegradation tests. The formulations of all samples are summarized in Table 1.

Simulated biodegradation test in river water

The biodegradation test under river water conditions was conducted in accordance with the protocol that we previously reported,[36] *via* measuring biochemical oxygen demand (BOD) using Oxitop-IDS (WTW, Germany). River water inoculum was collected from Gapcheon River, Daejeon, Republic of Korea (36° 21′51.13″ N, 127°21′55.73″ E). The water sample was sieved through a 45 μm filter to remove large organic particles, then stored for about 2 weeks with stirring. Nitrogen (NH_4Cl, 0.01 wt%) and phosphorus (KH_2PO_4, 0.05 wt%) nutrients were added just before the experiment. A 50 mg of M/P film (Na_2CO_3-1:1-W, *ca.* 2 × 2 cm^2), α-cellulose powder (positive control), and LDPE film (negative control) were used as substrates. The carbon content of materials was initially determined using an elemental analyzer (FLASH 2000, Thermo Fisher Scientific, United States; Table S1). Note that the carbon content data of LDPE and α-cellulose were obtained from the previous study,[37] which were determined by the same procedure. Blank samples without any substrate were also prepared. Each vessel containing 250 mL of river water medium and the sample was incubated in a climate chamber, maintaining 20 °C temperature and 30% relative humidity. BOD values of the samples were monitored for 30 days, and the degree of biodegradation was computed (eqn (1)):

$$\text{Biodegradation level } (\%) = \frac{\text{BOD}_{x,t} - \text{BOD}_{\text{blank},t}}{\rho_x \cdot \text{ThOD}} \times 100 \quad (1)$$

where $\text{BOD}_{x,t}$ (mg L^{-1}) represents BOD of the sample x at time t, ρ_x (g L^{-1}) denotes the sample concentration, and ThOD (mg g^{-1})

represents the theoretical BOD of the sample. All experiments were performed in triplicate.

Along with the BOD test, a microcosm test was conducted by immersing the Na_2CO_3-1:1-W film in 100 mL of either river water or deionized water, in bottles sealed with a filter cap to allow aeration. After 4 months of immersion, the samples were retrieved for surface morphology analysis. The samples were rinsed with deionized water and then soaked in a 2.5 w/v% glutaraldehyde solution for 24 hours to preserve the microbial structures. Subsequently, they were sequentially transferred into 70 vol% and 99 vol% ethanol solutions for dehydration, which were finally analyzed *via* SEM.

Simulated biodegradation test in soil

The biodegradation behavior of the Na_2CO_3-1:1-W film in the soil environment was analyzed by performing a laboratory experiment. The film (*ca.* 120 mg) was placed in a cubic polypropylene container (10 cm per side) with 200 g of dry soil, which was collected within the campus (36°22′3.98″ N, 127°21′40.87″ E). Prior to the experiment, the soil was filtered with a 2 mm sieve and supplemented with the following nutrients according to the ISO 17556 standard: KH_2PO_4 (0.04 g), $MgSO_4$ (0.02 g), $NaNO_3$ (0.08 g), $CO(NH_2)_2$ (0.04 g), and NH_4Cl (0.08 g). The container was closed with a cover equipped with a 0.2 μm air filter and placed in a commercial plant incubation chamber (Tiiun, LG Electronics, Republic of Korea) under controlled temperature (28 °C day/21 °C night) and a simulated light cycle (16 hours light/8 hours dark). After 5 weeks of incubation, the films were washed and dried, and their weight loss was measured in triplicate.

Ecotoxicity test

The potential ecotoxicity of the Na_2CO_3-1:1-W film was evaluated *via* an Italian ryegrass (*Lolium multiflorum*) germination test as per the OECD 208 standard[38] in triplicate. For each flowerpot, 40 mg of Na_2CO_3-1:1-W film was mixed with 40 g of loamy soil (Biophilia Co., Republic of Korea), and 20 ryegrass seeds were sown. After the initial two-day dark incubation, the pots were transferred to the commercial plant incubation chamber with a simulated light cycle (16 hours light and 8 hours dark). Water was provided every 2 days, while no additional nutrients were added. After three weeks of cultivation, germination rate and shoot length were recorded for each plant, and shoot wet mass was measured per pot. These values were compared to those of the blank samples (loamy soil without film materials).

Results and discussion

We fabricated mandarin peel/PVA blend films (M/P films) using an aqueous Na_2CO_3 solution as a mild base solvent (Fig. 1a). This pretreatment enables three key processes—partial hydrolysis of lignocellulose, dissolution of PVA, and blending—to occur simultaneously, thereby reducing both processing time and energy consumption. Notably, the pretreatment method used in this study avoids toxic chemicals and minimizes waste generation, ensuring a green fabrication process. Subsequently, we performed ultrasonication and washing as post-treatment steps (Fig. 1b), leading to significant improvements in mechanical, optical, and water-resistant properties. To maximize waste valorization efficiency, we used a high mandarin peel content (20–50 wt%) in all procedures, in contrast to previous studies that employed lower loadings. Although films could be produced using mandarin peel alone, they exhibited far weaker mechanical properties without additional treatments (*e.g.*, hot pressing). Therefore, PVA was incorporated to enhance the mechanical strength of the M/P films while maintaining biodegradability.

Effect of different pretreatment methods

In the first part of this study, we investigated the effects of different pretreatment methods to produce M/P films, with the

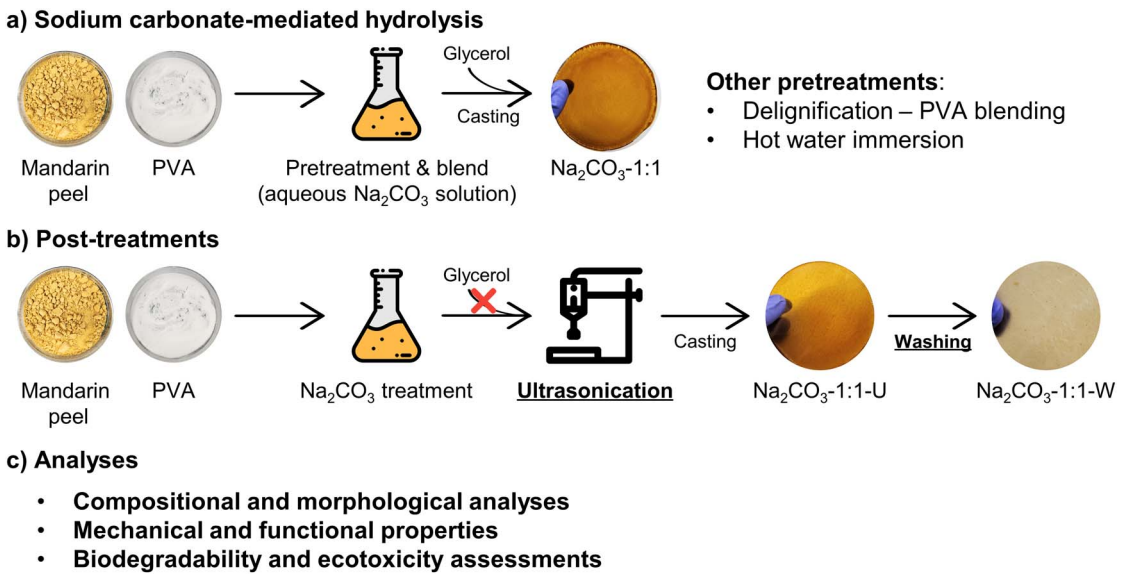

Fig. 1 Overview of the experimental scheme, including (a) Na_2CO_3 hydrolysis, (b) post-treatments (highlighted in bold), and (c) analytical methods.

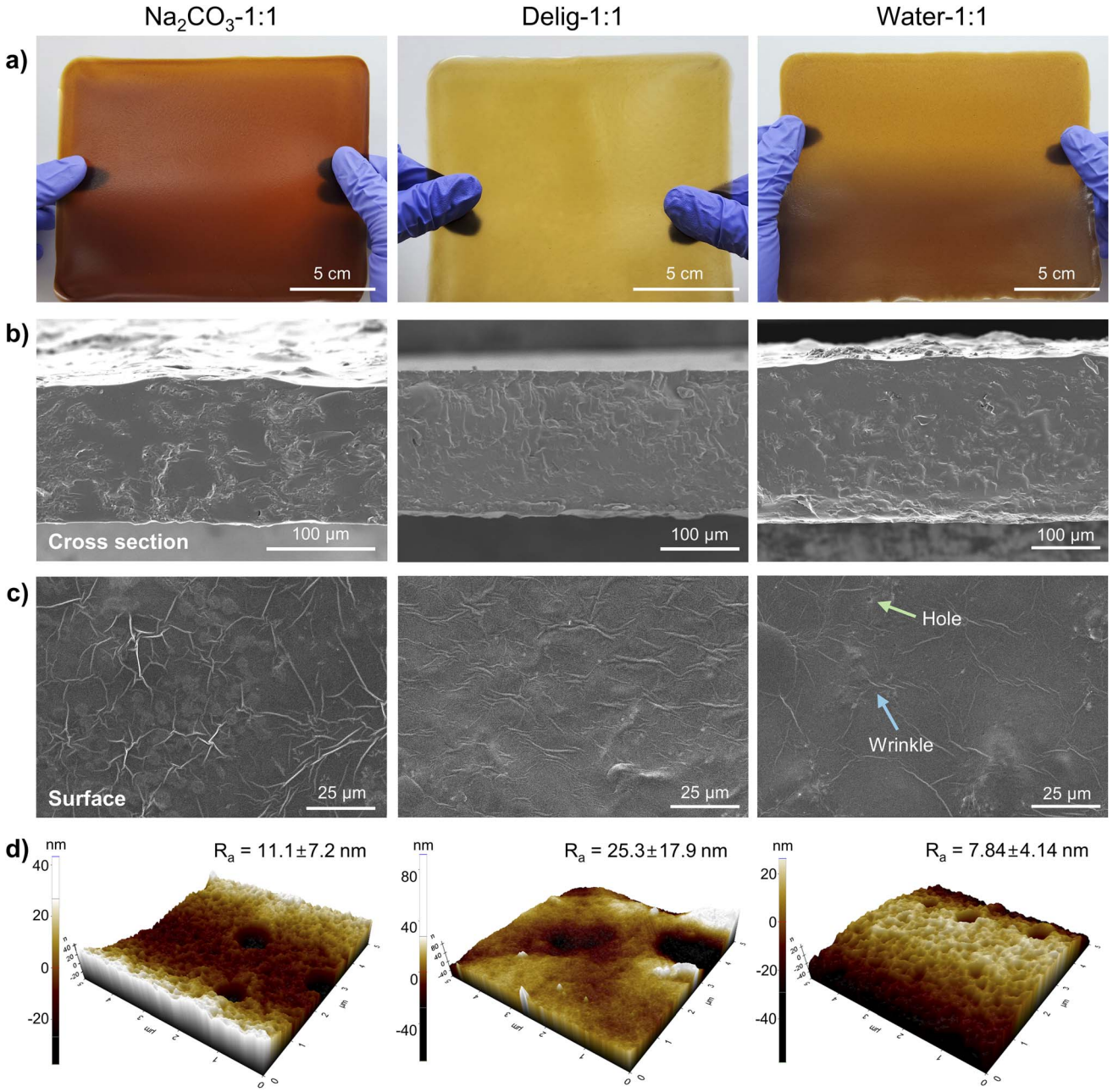

Fig. 2 (a) Digital photographs of the M/P films obtained from different pretreatment procedures. (b) Cross-sectional SEM images of the M/P films. (c) Surface SEM images of the M/P films (air-contacted side). The blue arrow indicates the wrinkle on the surface, where the green arrow indicates the hole on the surface. (d) Representative AFM images and the arithmetic mean roughness (R_a) obtained from three measurements.

M/P ratio fixed at 1 : 1. In addition to films prepared *via* mild base treatment (Na_2CO_3-1:1), comparative samples were prepared using two alternative approaches: a two-step delignification followed by PVA blending (Delig-1:1), and hot water suspension (Water-1:1), which served as a control (Fig. S2).

First, surface and cross-sectional SEM images of films were analyzed to examine the compatibility of natural polymers and PVA. All M/P films exhibited a homogeneous surface and semi-transparent appearance (Fig. 2a). Cross-sectional images of the M/P films (Fig. 2b) showed a homogeneous and dense structure, indicating good compatibility between PVA and the natural polymers. In addition, we assessed the surface smoothness of the M/P films, focusing on the air-contacted side, which refers to the surface exposed to air during the drying stage. The SEM images of the air-contacted surface (Fig. 2c) were generally smooth but exhibited some wrinkles, which may have resulted from slow and uneven drying under ambient conditions.[39] Further AFM analyses on the air-contacted surface confirmed a smooth morphology across all M/P films (Fig. 2d). The arithmetic mean roughness (R_a) of Na_2CO_3-1:1 and Water-1:1 was approximately 10 nm, which is comparable to that of most commercial plastic films, while Delig-1:1 exhibited a higher

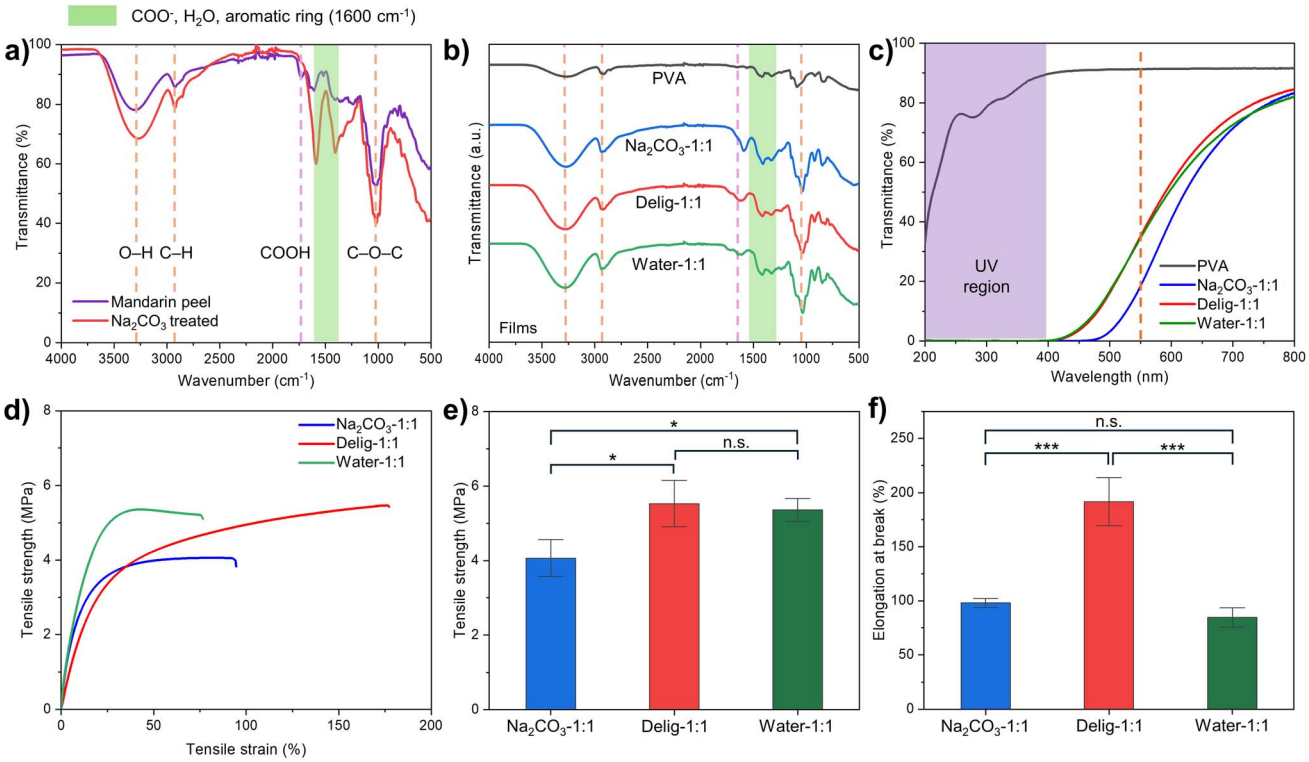

Fig. 3 Properties of the M/P films from different pretreatment methods. (a) FT-IR spectra of pristine and Na_2CO_3-treated mandarin peel. (b) FT-IR spectra of pure PVA and the M/P films. (c) UV-vis transmittance of pure PVA and the M/P films. The UV region is indicated by the purple-shaded region, and the orange dashed line indicates the transmittance at 550 nm. (d–f) Tensile properties of M/P films, along with statistical analyses of tensile strength and elongation at break. *: $p < 0.05$, ***: $p < 0.001$, n.s., not significant at the 95% confidence level.

roughness of 25.3 nm. Additionally, the substrate-contacted side, which was in direct contact with the substrate when dried, showed an even smoother structure (Fig. S4). Overall, all M/P film samples displayed smooth and homogeneous surface morphology, confirming the excellent compatibility between the polymers. However, the presence of multiple holes in the Water-1:1 sample suggests insufficient pretreatment, which may compromise its barrier properties.

To further elucidate the effect of Na_2CO_3 hydrolysis, we analyzed FT-IR spectra of pristine mandarin peel (powder) and Na_2CO_3-treated mandarin peel (film) without PVA incorporation (Fig. 3a). Both spectra exhibited characteristic peaks corresponding to cellulose, pectin, and lignin (Table S2), as additionally confirmed by compositional analysis (Table S3). After Na_2CO_3 treatment, the intensity of several peaks increased, indicating that hydrolysis occurred during the treatment. For example, the peaks at 3300 cm^{-1} and 1020 cm^{-1}, corresponding to the hydroxy group (–OH) and glycosidic bond (C–O–C), respectively (orange dashed lines in Fig. 3a), reflect functional groups in cellulose, pectin, and other natural polymers. Partial hydrolysis by Na_2CO_3 likely cleaved the glycosidic bonds or intermolecular bonds between the different natural polymers, intensifying these peaks. Hydrolysis of lignin can also produce additional hydroxy groups, as well as alkenyl (–C=C–) groups represented at 1600 cm^{-1}. These findings are in line with previous research on ammonium hydroxide (NH_4Cl)-mediated biomass hydrolysis.[23] Furthermore, carboxylic acids of pectin were deprotonated in the presence of the base, forming carboxylates, as evidenced by the peak shift from 1740 cm^{-1} (purple dashed line) to 1600 cm^{-1} and 1400 cm^{-1} (green shade in Fig. 3a).[40] Residual moisture in samples may also contribute to the increase in the peak at 1600 cm^{-1}. Taken together, the peak at 1600 cm^{-1} is attributed to alkenyl, ketone, and carboxylate groups, as well as water molecules, which are hardly distinguishable from each other. The M/P films obtained from different pretreatments resulted in similar intensified peaks at 3300, 1600, and 1020 cm^{-1}, which clearly distinct from the spectrum of the pure PVA film (Fig. 3b). We also conducted liquid-state ^{13}C NMR analysis using DMSO-d_6 as the solvent to further elucidate the molecular structure (Fig. 4b), comparing the results with a previous example of pectin-containing biomass.[41] Mandarin peel powder exhibited characteristic peaks corresponding to cellulose, pectin, and hemicellulose in the chemical shift region of 55–180 ppm. In the Na_2CO_3-1:1 film spectrum, most of these peaks were retained, although peaks in the far downfield region were slightly diminished. Further discussion on NMR results is provided in the subsequent section.

The optical properties of the film products, including UV-blocking properties and visible light transmittance, play a crucial role in practical applications such as packaging. The UV-blocking performance and optical transparency of M/P films were evaluated by UV-vis spectroscopy (Fig. 3c, Table S4). The pure PVA film showed high transparency, with a visible light transmittance of 91.3% at 550 nm, but showed inferior UV-

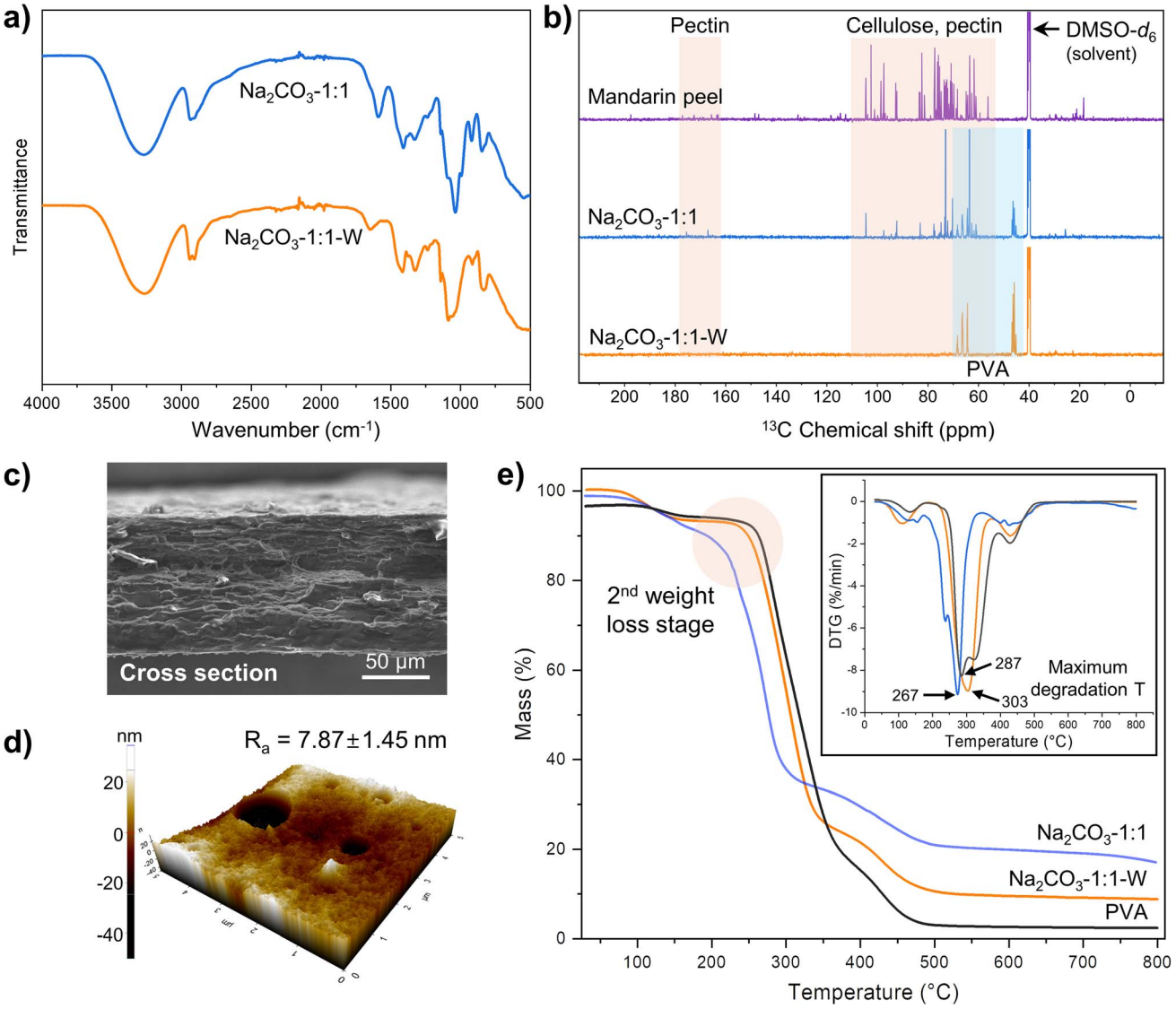

Fig. 4 Characterization of post-treated samples. (a) FT-IR spectra of Na_2CO_3-1:1 and Na_2CO_3-1:1-W. (b) Liquid ^{13}C NMR spectra of mandarin peel powder, Na_2CO_3-1:1, and Na_2CO_3-1:1-W films in DMSO-d_6. (c) Cross-sectional SEM image of Na_2CO_3-1:1-W. (d) A representative AFM image of Na_2CO_3-1:1-W. (e) TGA curves of PVA, Na_2CO_3-1:1, and Na_2CO_3-1:1-W. The orange circle indicates the second thermal degradation stage of interest (further analyzed in Fig. S5). The inset graph shows the differential TGA curves.

blocking properties. On the other hand, all M/P films exhibited exceptional UV-blocking properties, achieving nearly 100% of UV-A and UV-B blocking abilities. However, this improved UV protection came at the cost of reduced visible light transmittance compared to the pure PVA film. These phenomena can be explained by the presence of highly conjugated organic compounds, primarily lignin and polyphenols, in mandarin peel. These compounds contain a number of aromatic rings and alternating single and double carbon–carbon bonds, which absorb both UV and visible light. The degree of absorbance depends on the number and types of conjugated π orbitals within these molecules.[42,43] Notably, delignification led to a higher transmittance of Delig-1:1 at 550 nm (35.2%) than that of Na_2CO_3-1:1 (18.5%), while still maintaining high UV-blocking properties. We speculate that the remaining lignin or hydrolyzed organic compounds can reduce the visible light transmittance of the Na_2CO_3-1:1 film, since it did not undergo further purification or separation steps.

In the tensile test, all M/P films exhibited high elongation at break, ranging from 100 to 200%, due to the inherent high ductility of PVA and the presence of glycerol as a plasticizer (Fig. 3d). Among the samples, Delig-1:1 displayed the highest ductility, with a fracture strain twice as large as that of the other films (Fig. 3f). This increase in ductility is likely due to the removal of the rigid lignin structure, which enhances the flexibility of the polymer chains. On the other hand, tensile strength of the M/P films ranged from 4 to 6 MPa, where the Na_2CO_3-1:1 film showed slightly lower tensile strength than the other two M/P films (Fig. 3e). This reduction may be attributed to the lack of a separation step in the Na_2CO_3 pretreatment, leading to the presence of fractionated small molecules and residues, such as sugars and fractionated molecules. Additionally, while the

incorporation of glycerol facilitates easy peeling of the films, it also increases the moisture content, which in turn reduces tensile strength. This finding also aligns with previous research, showing that higher water content reduces the tensile strength of pure PVA films.[44] Based on these observations, we hypothesized that additional treatments could improve the optical and mechanical properties of the Na_2CO_3-1:1 film.

Effects of post-treatments on the chemical, thermal, and mechanical properties

To address the aforementioned drawbacks of the Na_2CO_3-1:1 film, two additional post-treatments were performed (Fig. 1b). First, ultrasonication was applied to enhance the hydrolysis of lignocellulose and promote homogeneous mixing with the natural polymers and PVA. Interestingly, ultrasonication also exhibited a plasticizing effect, eliminating the need for glycerol. Glycerol was initially used to reduce brittleness and facilitate film removal after drying; however, its tendency to absorb atmospheric moisture adversely affected the long-term stability of the films, as also reported elsewhere.[45] Given the plasticization effect of ultrasonication demonstrated in previous studies,[46,47] it could serve as a substitute for glycerol, though further supporting evidence is needed. In addition, the prepared M/P film (Na_2CO_3-1:1-U) was washed several times with water at room temperature and dried again, yielding the Na_2CO_3-1:1-W sample. Unlike the initial Na_2CO_3-1:1 film, the Na_2CO_3-1:1-U film prepared with ultrasonication was more easily washed due to its improved water stability. The washing step also removed hydrolysis residues and neutralized the pH. Consequently, these two post-treatments synergistically fostered the improvement of the mechanical, optical, and other functional properties of the M/P films.

Chemical and morphological characterization. The chemical composition of the M/P films after post-treatments was analyzed by FT-IR and ^{13}C NMR. From the FT-IR spectra (Fig. 4a), the only notable difference was the peak shift from 1600 cm^{-1} to 1640 cm^{-1}, which can be attributed to the absence of glycerol, pH neutralization of carbonyl group in pectin, and other related factors. In contrast, the ^{13}C NMR spectrum of Na_2CO_3-1:1-W dissolved in DMSO-d_6 was compared with those of mandarin peel powder and Na_2CO_3-1:1, revealing distinct differences (Fig. 4b). In mandarin peel, most polysaccharide-related peaks were observed in the chemical shift range of 55–180 ppm, corresponding to deshielded carbons bonded to oxygen atoms,[41] which were well retained in the spectrum of Na_2CO_3-1:1. However, several polysaccharide-related peaks disappeared after the post-treatments (in Na_2CO_3-1:1-W), resulting in the NMR spectrum closely resembling that of PVA. This observation seems somewhat contradictory to the FT-IR result of Na_2CO_3-1:1-W, which still exhibited characteristic peaks of polysaccharides and lignin in the wavenumber range of 1700–1000 cm^{-1}. Considering the low solubility of cellulose in DMSO (the NMR solvent) and the FT-IR results, the primary role of the post-treatments appears to be the removal of pectin and other residues. This finding aligns with a previous study in which ultrasonication was used for pectin extraction in water.[27] Meanwhile, the chemical structures of cellulose and PVA remain largely intact, although the physical interactions between the polymer chains may be intensified *via* ultrasonication. In addition, the smooth surface morphology was preserved after post-treatments, as confirmed by the cross-sectional SEM image and AFM data (Fig. 4c and d).

Thermal properties. The thermal stability of PVA film and M/P films (before and after the post-treatments) was analyzed using TGA (Fig. 4e). The TGA curves of the M/P films displayed three major weight loss stages, as detailed in the corresponding DTGA curve (inset in Fig. 4e). The first weight loss occurring around 120 °C corresponds to moisture evaporation from the films. The M/P films contained approximately 7–10% moisture, whereas the PVA film had a lower moisture content (~2.5%). The second weight loss stage observed at 250–350 °C is attributed to the degradation of PVA and pectin. Notably, the post-treated sample (Na_2CO_3-1:1-W) showed enhanced thermal stability compared to Na_2CO_3-1:1, as evidenced by an increase in onset temperature from 243 °C to 253 °C (Fig. S5). Furthermore, the maximum degradation temperature of Na_2CO_3-1:1-W was observed at 306 °C, representing a notable improvement of 36 °C over Na_2CO_3-1:1. We assume that this improvement in thermal stability is the consequence of the removal of water-soluble sugars, fractionated molecules, or pectin during post-treatments. Finally, the final weight loss stage resulted from the thermal degradation of cellulose. The residual mass percentage increased for both M/P films compared to neat PVA, suggesting improved thermal stability.

Influence of post-treatments on mechanical properties. The two aforementioned post-treatments led to a significant improvement in tensile properties. The tensile strength of the M/P film increased from 4.07 ± 0.50 MPa to 10.7 ± 0.2 MPa after ultrasonication and the exclusion of glycerol, which was further enhanced to 47.9 ± 9.5 MPa after the washing and drying process (Fig. 5a). This improvement is attributable to more effective lignocellulose hydrolysis and cellulose microfibrillation, removal of pectin and reaction residues, and improved physical blending between polymer chains. Notably, M/P films after post-treatments showed much higher tensile strength than either pure PVA or mandarin films (Fig. 5b), suggesting the synergistic effect between the natural polymers and PVA *via* hydrogen bonding. Furthermore, M/P films with different ratios of mandarin peel and PVA were examined, with the 1 : 2 blend ratio exhibiting the highest tensile strength (59.7 MPa). However, the difference with other blend ratios was not statistically significant ($p > 0.05$) (Fig. 5c). Moreover, a prepared Na_2CO_3-1:1-W strip could lift a 10 kg bottle, demonstrating the practical applicability of M/P films for packaging (Fig. 5f and Movie S1). In summary, the strength of the M/P films is comparable to that of most conventional plastics (Fig. 5e) and previously reported PVA/biomass films (Table S5).[22,48] Meanwhile, these M/P films exhibited moderate ductility (8.92–53.8%), which increased proportionally with PVA content (Fig. 5d). As a result, all M/P films were easily foldable and processable into various shapes (Fig. S6). Therefore, the M/P blend ratio can be tailored to balance between biomass valorization efficiency and film ductility (Table S4).

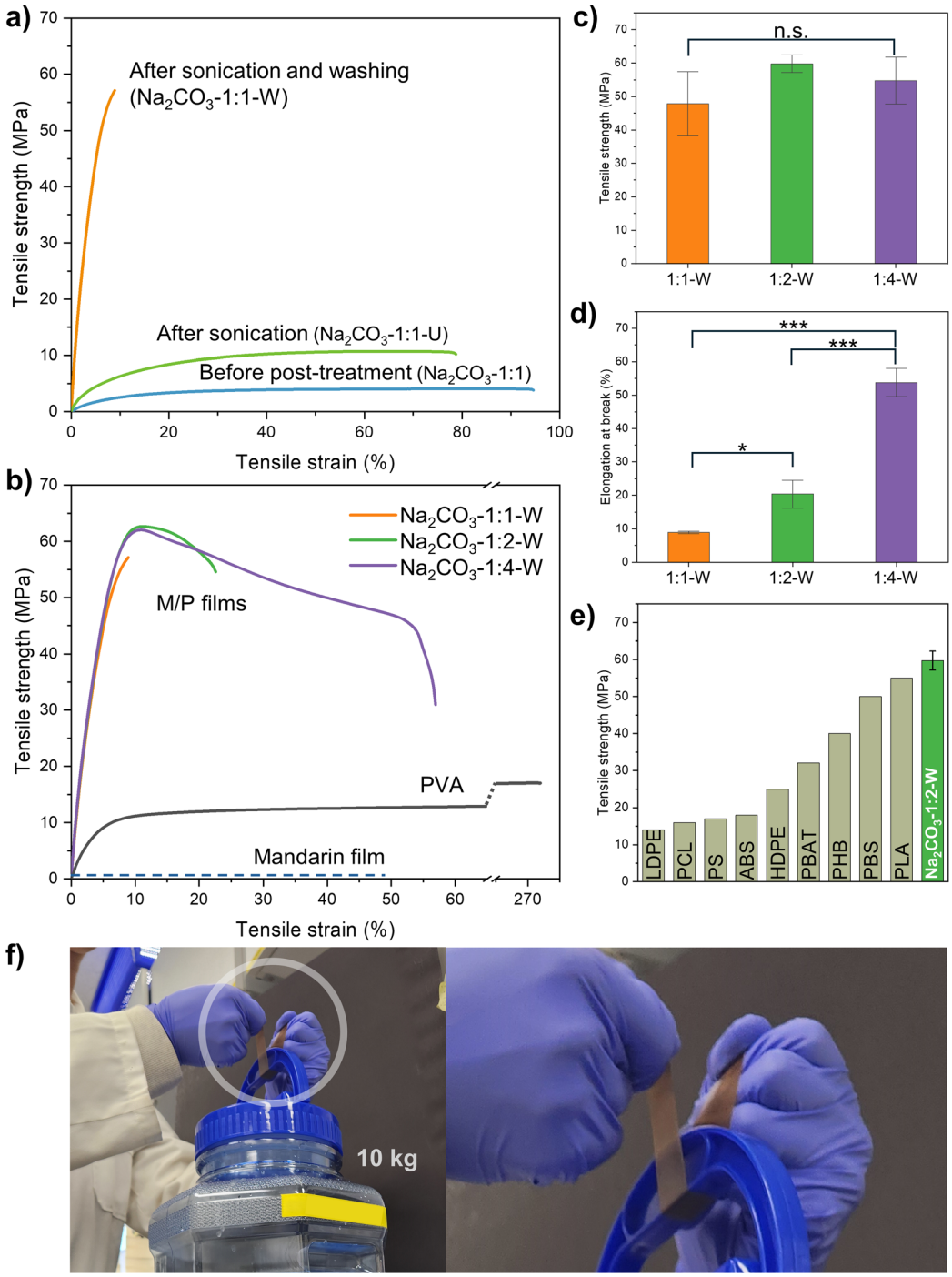

Fig. 5 Effect of post-treatments on the tensile properties of M/P films. (a) Stress–strain curves before and after each post-treatment step. (b–d) Tensile properties of post-treated films with different M/P blend ratios. (e) Comparison of the tensile strength of the Na_2CO_3-1:2-W film with conventional plastics: LDPE, PCL, PBAT, PHB, PBS, and PLA (ref. 48); PS, ABS, and HDPE (ref. 22). (f) Na_2CO_3-1:1-W strip lifting a 10 kg water bottle. *: $p < 0.05$, ***: $p < 0.001$, n.s., not significant at the 95% confidence level. Note that the stress–strain curves in (a) and (b) are the best representative data of each sample.

Functional properties of the M/P films

Optical properties. The post-treatments also improved the transmittance of the M/P films in the visible light region; for instance, Na_2CO_3-1:1-W exhibited 63.9% transmittance at 550 nm (Fig. 6a and Table S4). Meanwhile, the M/P films retained excellent UV-blocking properties even after post-treatments, with Na_2CO_3-1:1-W blocking 95.5% of the UV-A region and 99.6% of the UV-B region. The removal of reaction residues such as lignin fractions during the post-treatments might be the major contributing factor, while the decreased film thickness may also contribute to this effect. Although Na_2CO_3-1:2-W exhibited somewhat lower transparency, no

significant differences were observed between samples with different M/P ratios. Overall, these enhanced optical properties surpass those of similar PVA/biomass films (Table S5), highlighting the potential of these films for functional applications.

Antioxidant properties. Along with UV-blocking properties, antioxidant activity is also crucial for functional packaging, as it helps extend the shelf life of packaged products. Active antioxidants in mandarin peel, such as pectin and essential oils, can be directly incorporated into M/P films through the facile Na_2CO_3-mediated process. The antioxidant properties of mandarin peel powder, PVA film, and M/P films were examined by DPPH antioxidant assay. To facilitate the extraction of active compounds, samples were incubated in 50 vol% ethanol solution at 37 °C for 2 hours. The resulting supernatants were reacted with DPPH reagent for varying durations (5–120 minutes), and transmittance at 517 nm was measured for calculation of radical scavenging ability (Fig. 6b). Among the samples, mandarin peel powder exhibited the highest radical scavenging ability, reaching 60% within 5 minutes. Interestingly, the Na_2CO_3-1:1 film also demonstrated superior antioxidant activity, reaching up to 54% after 90 minutes. This result aligns with previous studies on pectin-containing antioxidant packaging films.[26,49,50] However, Na_2CO_3-1:1-W exhibited far lower antioxidant activity (14.8%), comparable to that of the pure PVA film. This finding suggests that pectin and other water-soluble antioxidants play a major role in antioxidant activity, and their removal through post-treatments could reduce the antioxidant capacity of the final products.

Oxygen and water vapor permeability. Gas barrier properties of films are crucial for food packaging applications. The PVA film is known for its excellent oxygen barrier properties, although it exhibits poor water vapor barrier properties under

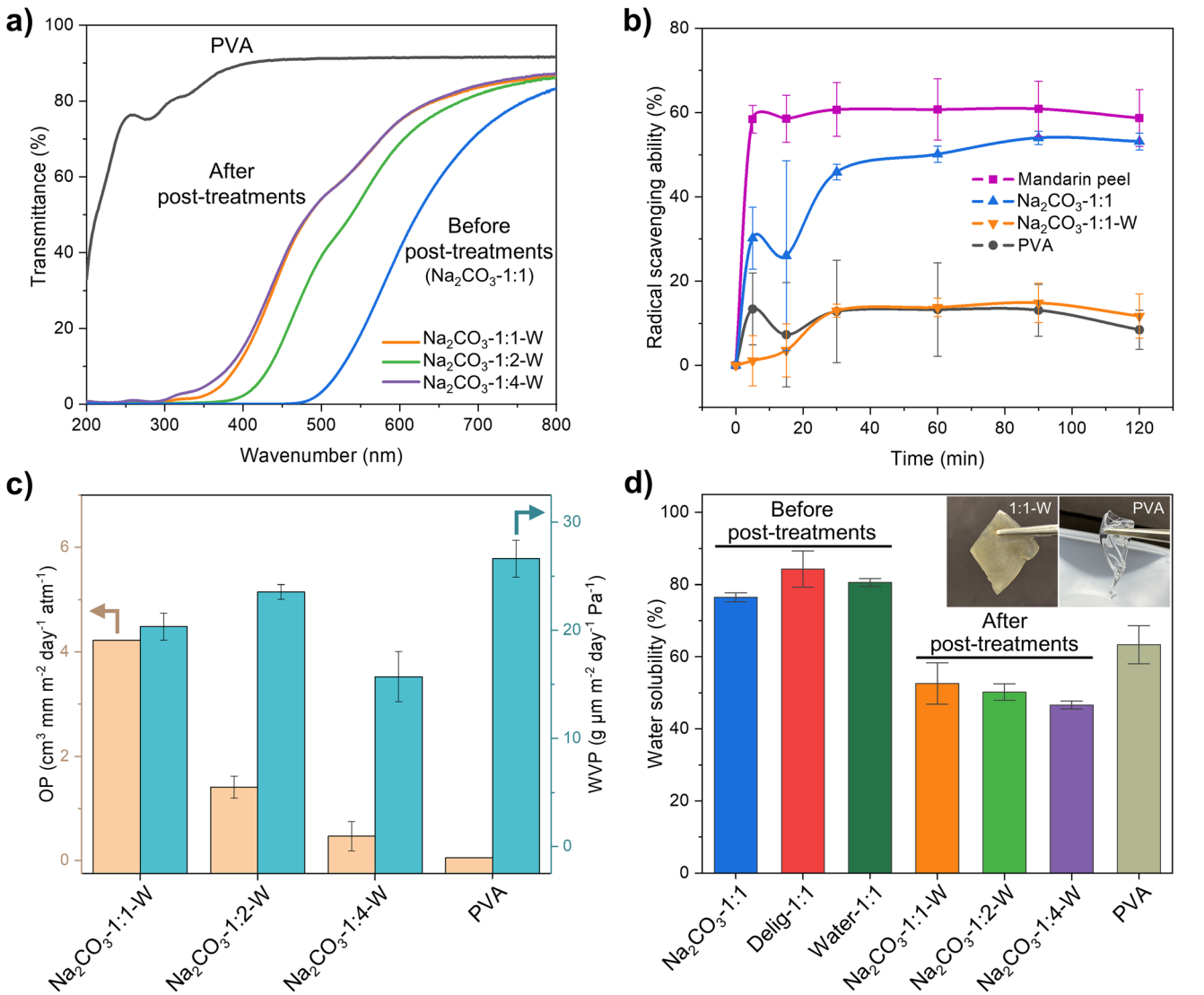

Fig. 6 (a) UV-vis transmittance of post-treated films in comparison with PVA and Na_2CO_3-1:1 (without post-treatment). (b) DPPH antioxidant assay results. (c) Oxygen permeability (OP) and water vapor permeability (WVP) of M/P and PVA films. (d) Water solubility of M/P and PVA films. Inset images are Na_2CO_3-1:1-W and PVA films after immersion in 60 °C water for 24 hours.

high temperature and humid conditions due to its hydrophilic nature. Therefore, we analyzed the effects of incorporating mandarin peel into PVA on both oxygen and water vapor barrier properties.

First, we analyzed oxygen barrier properties of pure PVA and M/P films according to the ASTM D3985 standard at 23 °C and 0% relative humidity. The pure PVA film showed the lowest oxygen permeability (OP) (0.053 ± 0.003 cm^3 mm m^{-2} day^{-1} atm^{-1}), demonstrating excellent oxygen barrier properties. The OP of M/P films increased with the content of mandarin peel, ranging from 0.47 to 4.22 cm^3 mm m^{-2} day^{-1} atm^{-1} (Fig. 6c). The incorporation of a relatively high concentration of mandarin peel (25–50%) might increase the porosity of the films or decrease the crystallinity of PVA, where a similar trend was also observed in a PVA/chitosan blend example.[51] Nevertheless, the M/P films exhibited excellent oxygen barrier properties, outperforming common polyethylene and polypropylene, which typically show OP values in the range of 50–200 cm^3 mm m^{-2} day^{-1} atm^{-1}.[52]

Next, we analyzed the water vapor permeability (WVP) of pure PVA and M/P films at 23 °C and 85% relative humidity. Interestingly, the M/P films presented lower WVP (15.7–23.5 g μm m^{-2} day^{-1} Pa^{-1}) compared to the neat PVA film (26.6 ± 1.7 g μm m^{-2} day^{-1} Pa^{-1}), indicating enhanced water barrier properties (Fig. 6c). The incorporation of cellulose and other natural compounds might create tortuous paths that hinder water molecule penetration, and cellulose might be less sensitive under humid conditions than PVA. Among the M/P films with different ratios, the Na_2CO_3-1:4-W film displayed the lowest WVP (15.7 ± 2.3 g μm m^{-2} day^{-1} Pa^{-1}). This suggests that the more homogeneous dispersion of the natural polymers in the PVA matrix can be achieved in lower mandarin peel loadings. Although the water vapor barrier properties of the M/P films are comparable to most biobased packaging materials, such as chitosan and alginate, they remain inferior to those of commercial packaging (*e.g.*, 0.05–0.1 g μm m^{-2} day^{-1} Pa^{-1} for LDPE).[53] Further optimization is needed for the successful adoption of these products.

Water stability. A common disadvantage of PVA and biobased polymers is their poor water resistance. Hence, we analyzed the M/P films' water contact angle and water solubility (at 60 °C). The water contact angle of the prepared M/P films ranged from 38.3° (Na_2CO_3-1:1-W) to 67.5° (Na_2CO_3-1:4-W) (Fig. S7). Interestingly, the contact angle of the M/P films increased with PVA content, exceeding that of the pure PVA film (42.3°) in some cases. However, all M/P films still remained hydrophilic, as their contact angles were below 90°. We attribute this hydrophilicity to the presence of cellulose, pectin, and PVA in the M/P films, while the contribution of hydrophobic substances is negligible. Additionally, surface roughness of the films (not assessed for Na_2CO_3-1:2-W and Na_2CO_3-1:4-W films) may have influenced the overall results. Next, the water stability of various M/P films was examined by immersing them in 60 °C water for 24 hours. The M/P films without post-treatments exhibited extremely weak water resistance, with a water solubility of ~80%. On the other hand, the water resistance of the M/P films was improved after post-treatments, as their solubility decreased to around 50%, surpassing that of PVA (Fig. 6d). The post-treated samples retained their original shape after immersion; however, the PVA film was swollen (inset images in Fig. 6d). It can be attributed to a possible physical cross-linking between cellulose and PVA *via* hydrogen bonds. The practical water stability of these films, *i.e.*, under ambient conditions, would exceed that observed in 60 °C water, which is beneficial for practical applications.

Biodegradability and ecotoxicity tests

PVA was selected as a blending component for mandarin peel due to its superior biodegradability in natural environments, particularly in aquatic systems. Therefore, we first evaluated the biodegradation behavior of the M/P film by simulating a river water environment in the laboratory. Bottom water was collected along with sediment, as the M/P films settle down in the water ($\rho > 1$). The biodegradability of the samples was assessed through BOD measurement, as BOD values indicate oxygen consumption by microorganisms during assimilation. By comparing the BOD values of sample-containing vessels with blank vessels, the biodegradability of the samples was quantitatively evaluated. Since the M/P film comprises PVA, cellulose, pectin, and other natural compounds, we estimated that its biodegradation rate would exceed that of the pure PVA film but be somewhat slower than that of pure cellulose. After 30 days of the biodegradation test, the Na_2CO_3-1:1-W film completely disintegrated, reaching a biodegradation level of 29.7 ± 10.2%, which indicates moderate biodegradability between that of the LDPE film and α-cellulose powder (Fig. 7a). Despite its lower surface area compared to powdered samples, the M/P film demonstrated excellent biodegradability in film form. These results are consistent with our previous studies; for example, PVA powder and cellulose powder biodegraded by 22.5% and 61.8%, respectively, in river water.[36] Similarly, PVA-coated kraft paper, composed of cellulose, PVA coating, and other additives, biodegraded by 59.2–81.6% for 111 days in seawater.[54] In addition, we performed a biodegradation test of the Na_2CO_3-1:1-W film in a soil environment. The film was slightly disintegrated after 6 weeks of incubation, showing some cracks and microbial colonization (Fig. S8). The mass of films was reduced by 30.4 ± 1.9%, indicating moderate biodegradation in soil. Given that both PVA and cellulose are known to degrade in ambient environments, the developed M/P films are expected to be readily biodegradable in diverse natural environments, posing minimal environmental impact.

In contrast, the M/P film did not fully disintegrate in the river water microcosm test after four months, likely due to the absence of mechanical stirring and nutrient supplementation. However, this provided an opportunity to examine the surface morphology of the films after microbial colonization. Indeed, biofilms were observed from the M/P film immersed in river water, whereas no visible biofilm formation was observed from the sample immersed in deionized water (Fig. 7b). The surface morphology of the two samples was further examined *via* SEM. Cracks and holes observed on the film immersed in river water provide evidence of microbial degradation. However, the film

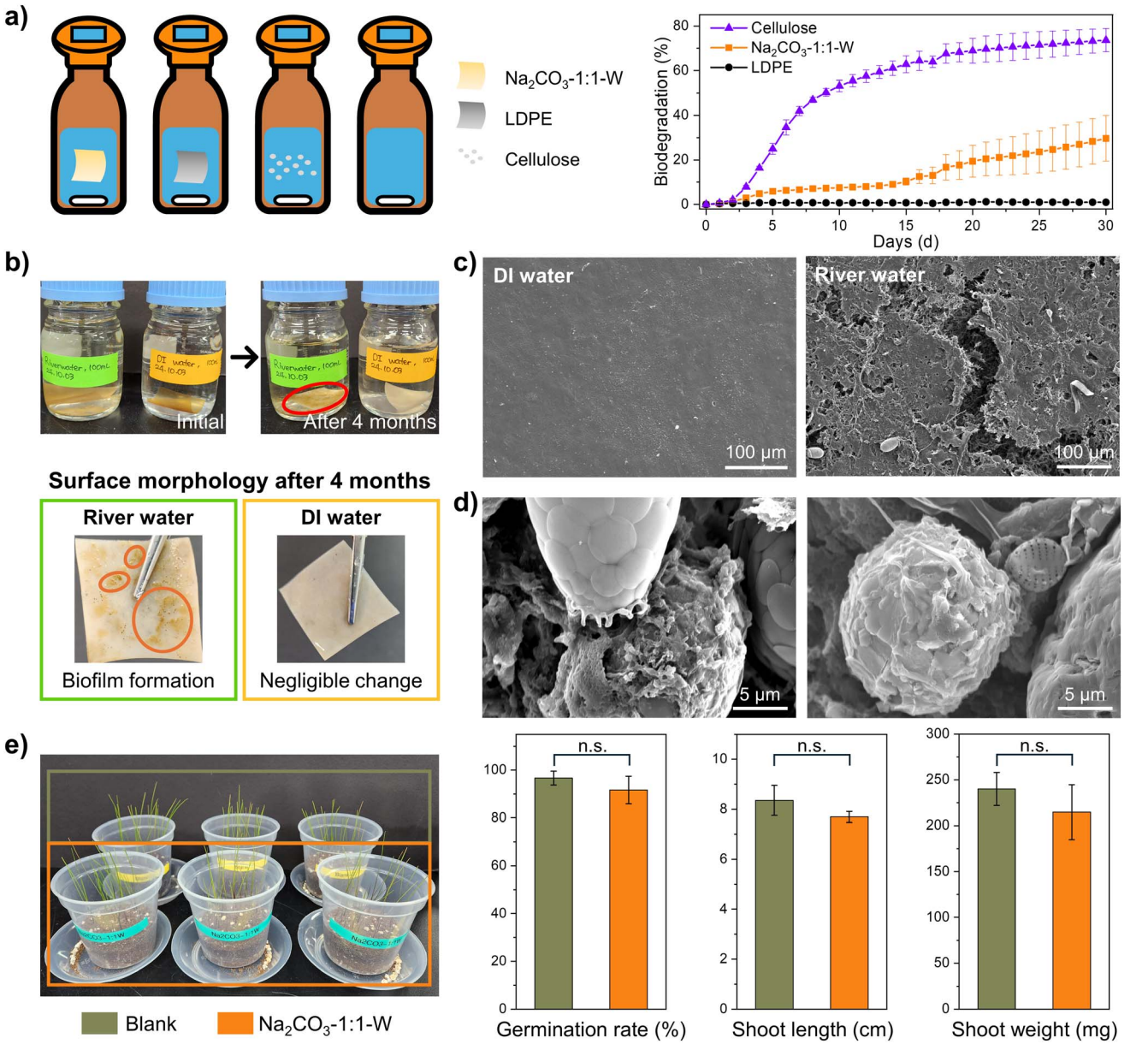

Fig. 7 End-of-life assessments of M/P films. (a) Biodegradation test under simulated river water conditions: BOD test setup (left) and biodegradation level (right). (b) Microcosm test in river water (left bottle) and deionized water (right bottle), showing microbial colonization in the river water sample (bottom left). (c) Surface morphology of two samples observed *via* SEM. (d) High-magnification SEM images of the sample immersed in river water. (e) Ecotoxicity test using ryegrass: results of germination rate, shoot length, and shoot weight per pot.

exposed to deionized water showed no such structural damage (Fig. 7c). In addition, various microorganisms, including amoebae, algae, fungi, and other microbial species, were identified (Fig. 7d, and S9), suggesting their potential involvement in the degradation process.

Finally, we conducted an ecotoxicity test utilizing ryegrass seeds in accordance with the OECD 208 standard. After three weeks of germination, we compared the germination rate, shoot length, and shoot weight per pot of Na_2CO_3-1:1-W-treated samples with those of the blank control group (Fig. 7e). No significant differences were observed between the two groups, indicating the negligible phytotoxicity of the M/P films. In contrast, our previous study reported that the use of a toxic metal salt ($NiCl_2$) as a positive control resulted in a significant 80–90% reduction in these parameters.[37]

Limitations and future research directions

Although our optimized M/P films have demonstrated strong mechanical and functional properties while remaining environmentally friendly, we acknowledge several limitations that warrant further investigation. These include the need for further optimization of feedstock selection and experimental

conditions, along with enhancing the water stability of the final products. For example, while we utilized locally-available mandarin peel waste as a feedstock, this approach could be extended to other region-specific agricultural residues rich in pectin, such as sugar beet waste and apple pomace.[55,56] In line with this, future studies will aim to further characterize the composition of natural polymers and bioactive compounds in such biomass waste, and to explore alternative pretreatment strategies and film-forming mechanisms tailored to specific biomass composition. Techno-economic and life cycle assessments will also be crucial to evaluate the economic feasibility of these approaches. Another key limitation is the relatively poor water barrier performance of our current films. To address this, post-coating processes using hydrophobic natural oils such as epoxidized corn oil[57] or sustainable crosslinking strategies[58] might be viable, without compromising biodegradability. Moreover, replacing the hydrophilic PVA component with another biodegradable polymer represents a feasible alternative, although it may require a different fabrication strategy.

Conclusions

We have developed a simple and cost-effective strategy to upcycle underutilized mandarin peel waste into biodegradable plastics, providing a sustainable alternative to conventional non-degradable plastics. In particular, Na_2CO_3 solution proved to be an efficient reagent in producing the mandarin peel/PVA (M/P) films by simultaneously facilitating partial hydrolysis of biomass, PVA dissolution, and blending. The functional properties of the films were further enhanced by additional post-treatments, including ultrasonication and washing. The optimized products demonstrated excellent tensile strength, UV-blocking abilities, antioxidant properties, and gas barrier performance, making them promising candidates for functional packaging or biodegradable mulch films. Furthermore, the in-depth biodegradation and ecotoxicity assessments provided clear evidence that the films pose no environmental harm, even under inadvertent environmental exposure. Overall, this strategy presents a unique waste-derived approach to tackling plastic pollution, aligning with the UN Sustainable Development Goals. Looking ahead, expanding the scope of waste-derived biodegradable plastic research to a broader range of agricultural residues, together with thorough economic assessments, will be essential for advancing sustainable material innovation. Through these efforts, we envision more efficient and eco-friendly waste valorization strategies for biodegradable plastic production, ultimately contributing to the realization of a circular economy.

Author contributions

Yongjun Cho: conceptualization, methodology, investigation, writing – original draft, writing – review & editing, visualization. Sunoo Hwang: methodology, investigation, writing – review & editing. Pham Thanh Trung Ninh: methodology, investigation, writing – review & editing. Youngju Kim: investigation, writing – review & editing, visualization. Shinhyeong Choe: investigation, methodology, writing – review & editing. Jaewook Myung: conceptualization, writing – review & editing, supervision, project administration, funding acquisition.

Conflicts of interest

There are no conflicts to declare.

Data availability

Additional characterization methods and results have been included in the supplementary information (SI). Supplementary information is available. See DOI: **https://doi.org/10.1039/d5su00465a**.

Acknowledgements

This research was supported by the National Research Foundation of Korea (NRF) grant funded by the Korea government (MSIT) (RS-2023-00209472 and RS-2024-00437656), Korea Institute of Planning and Evaluation for Technology in Food, Agriculture and Forestry (IPET) through Livestock Industrialization Technology Development Program, funded by Ministry of Agriculture, Food and Rural Affairs (MAFRA) (321089-5), and Korean Ministry of Land, Infrastructure and Transport (MOLIT) as Innovative Talent Education Program for Smartcity. This research was also funded by the Ministry of Oceans and Fisheries, Korea (20200104). Additionally, we appreciate Hoseong Moon and Yernazar Kuan, M.S. students in the Graduate School of Green Growth and Sustainability, KAIST, for their support in conducting experiments.

Notes and references

1 OECD, *Global Plastics Outlook: Policy Scenarios to 2060*, OECD Publishing, Paris, 2022, DOI: **10.1787/aa1edf33-en**.
2 S. B. Borrelle, J. Ringma, K. L. Law, C. C. Monnahan, L. Lebreton, A. McGivern, E. Murphy, J. Jambeck, G. H. Leonard, M. A. Hilleary, M. Eriksen, H. P. Possingham, H. De Frond, L. R. Gerber, B. Polidoro, A. Tahir, M. Bernard, N. Mallos, M. Barnes and C. M. Rochman, *Science*, 2020, **369**, 1515–1518, DOI: **10.1126/science.aba3656**.
3 A. S. Pottinger, R. Geyer, N. Biyani, C. C. Martinez, N. Nathan, M. R. Morse, C. Liu, S. Hu, M. de Bruyn and C. Boettiger, *Science*, 2024, **386**, 1168–1173, DOI: **10.1126/science.adr3837**.
4 D. Allen, S. Allen, S. Abbasi, A. Baker, M. Bergmann, J. Brahney, T. Butler, R. A. Duce, S. Eckhardt, N. Evangeliou, T. Jickells, M. Kanakidou, P. Kershaw, P. Laj, J. Levermore, D. J. Li, P. Liss, K. Liu, N. Mahowald, P. Masque, D. Materic, A. G. Mayes, P. McGinnity, I. Osvath, K. A. Prather, J. M. Prospero, L. E. Revell, S. G. Sander, W. J. Shim, J. Slade, A. Stein, O. Tarasova and S. Wright, *Nat. Rev. Earth Environ.*, 2022, **3**, 393–405, DOI: **10.1038/s43017-022-00292-x**.
5 J. G. Rosenboom, R. Langer and G. Traverso, *Nat. Rev. Mater.*, 2022, **7**, 117–137, DOI: **10.1038/s41578-021-00407-8**.

6 K. Ghosh and B. H. Jones, *ACS Sustainable Chem. Eng.*, 2021, **9**, 6170–6187, DOI: **10.1021/acssuschemeng.1c00801**.
7 S. Y. Choi, Y. Lee, H. E. Yu, I. J. Cho, M. Kang and S. Y. Lee, *Nat. Microbiol.*, 2023, **8**, 2253–2276, DOI: **10.1038/s41564-023-01529-1**.
8 J. M. G. Alcantara, F. Distante, G. Storti, D. Moscatelli, M. Morbidelli and M. Sponchioni, *Biotechnol. Adv.*, 2020, **42**, 107582, DOI: **10.1016/j.biotechadv.2020.107582**.
9 B. X. Wang, Y. Cortes-Peña, B. P. Grady, G. W. Huber and V. M. Zavala, *ACS Sustainable Chem. Eng.*, 2024, **12**, 9156–9167, DOI: **10.1021/acssuschemeng.4c01842**.
10 S. Choe, Y. Kim, Y. Won and J. Myung, *Front. Chem.*, 2021, **9**, 671750, DOI: **10.3389/fchem.2021.671750**.
11 C. Espro, E. Paone, F. Mauriello, R. Gotti, E. Uliassi, M. L. Bolognesi, D. Rodríguez-Padrón and R. Luque, *Chem. Soc. Rev.*, 2021, **50**, 11191–11207, DOI: **10.1039/d1cs00524c**.
12 K. Lee, Y. Jing, Y. Wang and N. Yan, *Nat. Rev. Chem.*, 2022, **6**, 635–652, DOI: **10.1038/s41570-022-00411-8**.
13 C. G. Otoni, H. M. C. Azeredo, B. D. Mattos, M. Beaumont, D. S. Correa and O. J. Rojas, *Adv. Mater.*, 2021, **33**, 2102520, DOI: **10.1002/adma.202102520**.
14 J. S. Yaradoddi, N. R. Banapurmath, S. V. Ganachari, M. E. M. Soudagar, A. M. Sajjan, S. Kamat, M. Mujtaba, A. S. Shettar, A. E. Anqi and M. R. Safaei, *J. Mater. Res. Technol.*, 2022, **17**, 3186–3197, DOI: **10.1016/j.jmrt.2021.09.016**.
15 Y. Cho, P. T. T. Ninh, S. Hwang, S. Choe and J. Myung, *ACS Mater. Lett.*, 2025, **7**, 1563–1592, DOI: **10.1021/acsmaterialslett.4c02591**.
16 S. Zhang, X. Zhang, X. Wan, H. Zhang and J. Tian, *Carbohydr. Polym.*, 2023, **321**, 121290, DOI: **10.1016/j.carbpol.2023.121290**.
17 Y. C. Gorur, P. A. Larsson and L. Wågberg, *Biomacromolecules*, 2020, **21**, 3479, DOI: **10.1021/acs.biomac.0c00997**.
18 M. A. Martins, E. M. Teixeira, A. C. Corrêa, M. Ferreira and L. H. C. Mattoso, *J. Mater. Sci.*, 2011, **46**, 7858–7864, DOI: **10.1007/s10853-011-5767-2**.
19 S. Sankhla, H. H. Sardar and S. Neogi, *Carbohydr. Polym.*, 2021, **251**, 117030, DOI: **10.1016/j.carbpol.2020.117030**.
20 M. H. Hemida, H. Moustafa, S. Mehanny, M. Morsy, A. Dufresne, E. N. A. Rahman and M. M. Ibrahim, *Heliyon*, 2023, **9**, e16436, DOI: **10.1016/j.heliyon.2023.e16436**.
21 Q. Xia, C. Chen, Y. Yao, J. Li, S. He, Y. Zhou, T. Li, X. Pan, Y. Yao and L. Hu, *Nat. Sustain.*, 2021, **4**, 627–635, DOI: **10.1038/s41893-021-00702-w**.
22 S. Zhang, Q. Fu, H. Li, P. Wu, G. I. N. Waterhouse, Y. Li and S. Ai, *Chem. Eng. J.*, 2023, **463**, 142452, DOI: **10.1016/j.cej.2023.142452**.
23 D. Merino and A. Athanassiou, *Chem. Eng. J.*, 2023, **454**, 140171, DOI: **10.1016/j.cej.2022.140171**.
24 J. D. Estrada-Sotomayor, L. Lopusiewicz, E. Lizundia, S. Guenther and D. Merino, *Green Chem.*, 2025, **27**, 4587–4602, DOI: **10.1039/d5gc00643k**.
25 M. Shorbagi, N. M. Fayek, P. Shao and M. A. Farag, *Food Biosci.*, 2022, **47**, 101699, DOI: **10.1016/j.fbio.2022.101699**.
26 D. Yun, Z. Wang, C. Li, D. Chen and J. Liu, *Food Biosci.*, 2023, **51**, 102319, DOI: **10.1016/j.fbio.2022.102319**.
27 C. M. Chandrasekar, D. Carullo, F. Saitta, H. Krishnamachari, T. Bellesia, L. Nespoli, E. Caneva, C. Baschieri, M. Signorelli, A. G. Barbiroli, D. Fessas, S. Farris and D. Romano, *Carbohydr. Polym.*, 2024, **344**, 122539, DOI: **10.1016/j.carbpol.2024.122539**.
28 E. Chiellini, P. Cinelli, S. H. Imam and L. Mao, *Biomacromolecules*, 2001, **2**, 1029–1037, DOI: **10.1021/bm010084j**.
29 S. Rathinavel and S. S. Saravanakumar, *J. Nat. Fibers*, 2021, **18**, 2045–2054, DOI: **10.1080/15440478.2019.1711285**.
30 D. U. Pascoli, A. Dichiara, E. Roumeli, R. Gustafson and R. Bura, *Carbohydr. Polym.*, 2022, **295**, 119857, DOI: **10.1016/j.carbpol.2022.119857**.
31 P. K. Panda, K. Sadeghi and J. Seo, *Food Packag. Shelf Life*, 2022, **33**, 100904, DOI: **10.1016/j.fpsl.2022.100904**.
32 P. Terzioglu, F. Guney, F. N. Parin, I. Sen and S. Tuna, *Food Packag. Shelf Life*, 2021, **30**, 100742, DOI: **10.1016/j.fpsl.2021.100742**.
33 S. Regina, T. Poerio, R. Mazzei, C. Sabia, R. Iseppi and L. Giorno, *Eur. Polym. J.*, 2022, **172**, 111193, DOI: **10.1016/j.eurpolymj.2022.111193**.
34 H. Moustafa, A. M. Karmalawi and A. M. Youssef, *Environ. Nanotechnol., Monit. Manage.*, 2021, **16**, 100482, DOI: **10.1016/j.enmm.2021.100482**.
35 C. M. Zhao, X. H. Gong, X. T. Lin, C. Q. Zhang and Y. Wang, *Carbohydr. Polym.*, 2023, **321**, 121303, DOI: **10.1016/j.carbpol.2023.121303**.
36 Y. Kim, S. Choe, Y. Cho, H. Moon, H. Shin, J. Seo and J. Myung, *Sci. Total Environ.*, 2024, **953**, 176129, DOI: **10.1016/j.scitotenv.2024.176129**.
37 A. Camus, S. Choe, C. Bour-Cardinal, J. Isasmendi, Y. Cho, Y. Kim, C. V. Irimia, C. Yumusak, M. Irimia-Vladu, D. Rho, J. Myung and C. Santato, *Commun. Mater.*, 2024, **5**, 173, DOI: **10.1038/s43246-024-00592-3**.
38 OECD, *Test No. 208: Terrestrial Plant Test: Seedling Emergence and Seedling Growth Test*, OECD Publishing, Paris, 2006, DOI: **10.1787/9789264070066-en**.
39 Y. Wu, X. Luo, W. Li, R. Song, J. Li, Y. Li, B. Li and S. Liu, *Food Chem.*, 2016, **197**, 250–256, DOI: **10.1016/j.foodchem.2015.10.127**.
40 Y. Wandee, D. Uttapap, P. Mischnick and V. Rungsardthong, *Food Chem.*, 2021, **348**, 129078, DOI: **10.1016/j.foodchem.2021.129078**.
41 D. Merino, R. Simonutti, G. Perotto and A. Athanassiou, *Green Chem.*, 2021, **23**, 5956–5971, DOI: **10.1039/d1gc01316e**.
42 D. Wang, Y. Gu, S. Feng, W. Yang, H. Dai, H. Xiao and J. Han, *Green Chem.*, 2023, **25**, 9020–9044, DOI: **10.1039/d3gc02908e**.
43 H. Shao, Y. Zhang, H. Pan, Y. Jiang, J. Qi, H. Xiao, S. Zhang, T. Lin, L. Tu and J. Xie, *Int. J. Biol. Macromol.*, 2022, **207**, 917–926, DOI: **10.1016/j.ijbiomac.2022.03.183**.
44 L. Li, X. Xu, L. Liu, P. Song, Q. Cao, Z. Xu, Z. Fang and H. Wang, *Polymer*, 2021, **213**, 123330, DOI: **10.1016/j.polymer.2020.123330**.
45 A. Jones, M. A. Zeller and S. Sharma, *Prog. Biomater.*, 2013, **2**, 12, DOI: **10.1186/2194-0517-2-12**.

46 W. Wu, L. Pan, B. Li, X. He and B. Jiang, *Polym. Test.*, 2023, **118**, 107909, DOI: **10.1016/j.polymertesting.2022.107909**.
47 X. Liang, Y. J. Liu, S. G. Chen, J. Ma, X. Y. Wu, H. Y. Shi, L. Y. Fu and B. Xu, *J. Manuf. Process.*, 2020, **56**, 180–188, DOI: **10.1016/j.jmapro.2020.04.086**.
48 G. X. Wang, D. Huang, J. H. Ji, C. Völker and F. R. Wurm, *Adv. Sci.*, 2021, **8**, 2001121, DOI: **10.1002/advs.202001121**.
49 S. Zhang, X. Cheng, W. Yang, Q. Fu, F. Su, P. Wu, Y. Li, F. Wang, H. Li and S. Ai, *Bioresour. Technol.*, 2024, **406**, 131074, DOI: **10.1016/j.biortech.2024.131074**.
50 D. Merino, L. Bertolacci, U. C. Paul, R. Simonutti and A. Athanassiou, *ACS Appl. Mater. Interfaces*, 2021, **13**, 38688–38699, DOI: **10.1021/acsami.1c09433**.
51 J. Ding, R. Zhang, S. Ahmed, Y. W. Liu and W. Qin, *Molecules*, 2019, **24**, 1408, DOI: **10.3390/molecules24071408**.
52 J. W. Wang, D. J. Gardner, N. M. Stark, D. W. Bousfield, M. Tajvidi and Z. Y. Cai, *ACS Sustainable Chem. Eng.*, 2018, **6**, 49–70, DOI: **10.1021/acssuschemeng.7b03523**.
53 J. Y. Long, W. Y. Zhang, M. Z. Zhao and C. Q. Ruan, *Carbohydr. Polym.*, 2023, **321**, 121267, DOI: **10.1016/j.carbpol.2023.121267**.
54 S. Choe, S. You, K. Park, Y. Kim, J. Park, Y. Cho, J. Seo, H. Yang and J. Myung, *Green Chem.*, 2024, **26**, 8230–8241, DOI: **10.1039/d4gc00618f**.
55 M. C. Edwards and J. Doran-Peterson, *Appl. Microbiol. Biotechnol.*, 2012, **95**, 565–575, DOI: **10.1007/s00253-012-4173-2**.
56 J. Huo, Z. Y. Wang, P. Lauri, J. D. Medrano-García, G. Guillén-Gosálbez and S. Hellweg, *Environ. Sci. Technol.*, 2024, **58**, 13748–13759, DOI: **10.1021/acs.est.4c03005**.
57 S. Thakur, M. Misra and A. K. Mohanty, *ACS Sustainable Chem. Eng.*, 2019, **7**, 8766–8774, DOI: **10.1021/acssuschemeng.9b00689**.
58 Z. L. Jiang, K. M. Cheung and T. Ngai, *RSC Sustainability*, 2024, **2**, 139–152, DOI: **10.1039/d3su00219e**.